

An Efficient Proximal Gradient Method for General Structured Sparse Learning

Xi Chen

Qihang Lin

Seyoung Kim

Jaime G. Carbonell

Eric P. Xing

CARNEGIE MELLON UNIVERSITY
PITTSBURGH, PA 15213, USA

XICHEN@CS.CMU.EDU

QIHANGL@ANDREW.CMU.EDU

SSSYKIM@CS.CMU.EDU

JGC@CS.CMU.EDU

EPXING@CS.CMU.EDU

Editor:

Abstract

We study the problem of estimating high dimensional regression models regularized by a structured-sparsity-inducing penalty that encodes prior structural information on either input or output sides. We consider two widely adopted types of such penalties as our motivating examples: 1) overlapping-group-lasso penalty, based on the ℓ_1/ℓ_2 mixed-norm penalty, and 2) graph-guided fusion penalty. For both types of penalties, due to their non-separability, developing an efficient optimization method has remained a challenging problem. In this paper, we propose a general optimization approach, called smoothing proximal gradient method, which can solve the structured sparse regression problems with a smooth convex loss and a wide spectrum of structured-sparsity-inducing penalties. Our approach combines the smoothing technique and the proximal gradient method. It achieves a convergence rate significantly faster than the standard first-order method, subgradient method, and is much more scalable than the most widely used interior-point method. The efficiency and scalability of our method are demonstrated on both simulated and real genetic datasets.

Keywords: Smoothing Proximal Gradient, Structured Sparsity, Overlapping Group Lasso, Graph-guided Fused Lasso

1. Introduction

The problem of high-dimensional sparse feature learning arises in many areas in science and engineering. In a typical setting, the input lies in a high-dimensional space, and one is interested in selecting a small number of input variables that influence the output. A popular approach to achieve this goal is to jointly optimize the fitness loss function with a non-smooth ℓ_1 -norm penalty (e.g., lasso (Tibshirani, 1996)) that shrinks the coefficients of the irrelevant input variables to zero. However, this approach is limited in that it treats each input as independent of each other and hence is incapable of capturing any structural information among input variables. Recently, various extensions of the lasso penalty have been introduced to take advantage of the prior knowledge of the structure among inputs to encourage closely related inputs to be selected jointly (Yuan and Lin, 2006; Tibshirani and Saunders,

2005; Jenatton et al., 2009). Similar ideas have also been explored to leverage the output structures in multivariate regression, where one is interested in estimating multiple related functional mappings from a common input space to multiple outputs (Obozinski et al., 2009). In this case, the structure over the outputs is available as prior knowledge, and the closely related outputs according to this structure are encouraged to share a similar set of relevant inputs (Kim and Xing, 2010). Despite these progress, developing an efficient optimization method for solving the convex optimization problems resulting from the *structured-sparsity-inducing penalty functions* has remained a challenge. In this paper, we focus on the problem of developing efficient optimization methods that can handle a broad set of structured-sparsity-inducing penalties with complex structures.

When the structure to be imposed has a relatively simple form, such as non-overlapping groups over variables (e.g., group lasso Yuan and Lin (2006)), or a linear-ordering (a.k.a., chain) of variables (e.g., fused lasso (Tibshirani and Saunders, 2005)), efficient optimization methods have been developed. For example, under group lasso (Yuan and Lin, 2006), due to the separability among groups, a *proximal operator*¹ associated with the penalty can be computed in a closed-form; thus, a number of composite gradient methods (Beck and Teboulle, 2009; Nesterov, 2007; Liu et al., 2009) that leverage the proximal operator as a key step (so-called “proximal gradient method”) can be directly applied. For fused lasso, although the penalty is not separable, a coordinate descent algorithm was shown feasible by explicitly leveraging on the linear ordering of the inputs (Friedman et al., 2007).

In order to handle a more general class of structures such as tree or graph, various models that further extend group lasso and fused lasso have been proposed. While the standard group lasso assumes groups are separated, *overlapping group lasso*, which introduces overlaps among groups so that each input can belong to multiple groups, allows us to incorporate more complex prior knowledge on the structure (Jenatton et al., 2009). As for fused lasso, *graph-guided fused lasso* extends the chain structure to a general graph, where the fusion penalty is applied to each edge of the graph (Kim et al., 2009). However, due to the non-separability of the penalty that arises from overlapping groups or graphs, the fast optimization method for the standard group lasso or fused lasso cannot be easily applied (e.g. no closed-form solution of the proximal operator). In principle, generic solvers such as the interior-point methods (IPM) could always be used to solve either a second-order cone programming (SOCP) or a quadratic programming (QP) formulation of the aforementioned problems, such approaches are computationally prohibitive even for problems of moderate size. Very recently, this problem has received excellent attentions from a number of papers (Jenatton et al., 2010; Mairal et al., 2010; Duchi and Singer, 2009; Liu et al., 2010; Hoeffling, 2009) which all strived to provide clever solutions to various subclasses of the structured-sparsity-inducing penalties; but as we survey in Section 2, they are still shy of reaching a simple, unified, and general solution to a broad class of structured sparse regression problems.

In this paper, we propose a generic optimization approach, the smoothing proximal gradient method, for dealing with a variety of structured-sparsity-inducing penalties, using overlapping-group-lasso penalty and graph-guided fusion penalty as motivating examples. Although these two types of penalties are seemingly very different, we show that it is

1. The proximal operator associated with the penalty is defined as $\arg \min_{\beta} \frac{1}{2} \|\beta - \mathbf{v}\|_2^2 + P(\beta)$, where \mathbf{v} is any given vector and $P(\beta)$ is the non-smooth penalty.

possible to decouple the non-separable terms in both penalties via the dual norm; and reformulate them into a common form to which the proposed method can be applied. We call this approach “smoothing” proximal gradient method because instead of optimizing the original problem directly as in other proximal gradient methods, we introduce a *smooth* approximation of the structured-sparsity-inducing penalty using the smoothing technique from (Nesterov, 2005). Then, we solve the approximation problem by the first-order proximal gradient method: fast iterative shrinkage-thresholding algorithm (FISTA)(Beck and Teboulle, 2009). It achieves $O(\frac{1}{\epsilon})$ convergence rate for a desired accuracy ϵ . Below, we summarize the main advantages of this approach.

- (a) It is a first-order method, as it uses only the gradient information. Thus, it is significantly more scalable than IPM for SOCP or QP. Since it is gradient-based, it allows warm restarts, thereby potentiates solving the problem along the entire regularization path (Friedman et al., 2007).
- (b) It is applicable to a wide class of optimization problems with a smooth convex loss and a non-smooth non-separable structured sparsity-inducing penalty. The mixed-norm penalties as in overlapping-group-lasso and graph-guided fusion penalty are only examples for demonstration.
- (c) Theoretically, it enjoys a convergence rate of $O(\frac{1}{\epsilon})$, which dominates that of standard first-order method and subgradient method with rate $O(\frac{1}{\epsilon^2})$.
- (d) It is applicable to both uni- and multi-variate regression, with structures on either (or both) inputs/outputs.
- (e) Easy to implement with a few lines of MATLAB code.

The rest of this paper is organized as follows. In Section 2, we present the of overlapping group lasso and graph-guided fused lasso and discuss the existing optimization methods in the literature. In Section 3, we present the smoothing proximal gradient method along with complexity results. In Section 4, we present the generalization of this algorithm to the setting of the multivariate regression. In Section 5, we present numerical results on both simulated and real datasets, followed by conclusions in Section 6. Throughout the paper, we will discuss overlapping-group-lasso and graph-guided fusion penalties in parallel to illustrate how the smoothing proximal gradient method can be used to solve the corresponding optimization problems.

2. Background: Linear Regression Regularized by Structured-sparsity-inducing Penalties and Related Optimization Methods

We begin with a brief review of the high-dimensional linear regression model regularized by structured-sparsity-inducing penalties. To better position the proposed method, we also provide a survey of latest developments of efficient algorithms for solving subclasses of structured sparse regression problems.

Let $\mathbf{X} \in \mathbb{R}^{N \times J}$ denote the input data for N samples, where each sample lies in J dimensional space, and $\mathbf{y} \in \mathbb{R}^{N \times 1}$ be the output data. We assume a linear regression

Table 1: Comparisons of different first-order methods for optimizing mixed-norm based overlapping-group-lasso penalties.

Method	No overlap ℓ_1/ℓ_2	No overlap ℓ_1/ℓ_∞	Overlap Tree ℓ_1/ℓ_2	Overlap Tree ℓ_1/ℓ_∞	Overlap Arbitrary ℓ_1/ℓ_2	Overlap Arbitrary ℓ_1/ℓ_∞
Projection (Liu et al., 2009)	$O(\frac{1}{\sqrt{\epsilon}})$, $O(J)$	$O(\frac{1}{\sqrt{\epsilon}})$, $O(J \log J)$	N.A.	N.A.	N.A.	N.A.
Coordinate Ascent (Jenatton et al., 2010; Liu and Ye, 2010b)	$O(\frac{1}{\sqrt{\epsilon}})$, $O(J)$	$O(\frac{1}{\sqrt{\epsilon}})$, $O(J \log J)$	$O(\frac{1}{\sqrt{\epsilon}})$, $O(\sum_{g \in \mathcal{G}} g)$	$O(\frac{1}{\sqrt{\epsilon}})$, $O(\sum_{g \in \mathcal{G}} g \log g)$	N.A.	N.A.
Network Flow (Mairal et al., 2010)	N.A.	$O(\frac{1}{\sqrt{\epsilon}})$, quadratic min-cost flow	N.A.	$O(\frac{1}{\sqrt{\epsilon}})$, quadratic min-cost flow	N.A.	$O(\frac{1}{\sqrt{\epsilon}})$, quadratic min-cost flow
FOBOS (Duchi and Singer, 2009)	$O(\frac{1}{\epsilon})$, $O(J)$	$O(\frac{1}{\epsilon})$, $O(J \log J)$	$O(\frac{1}{\epsilon})$, $O(\sum_{g \in \mathcal{G}} g)$	$O(\frac{1}{\epsilon})$, $O(\sum_{g \in \mathcal{G}} g \log g)$	$O(\frac{1}{\epsilon^2})$, $O(\sum_{g \in \mathcal{G}} g)$ (subgradient)	$O(\frac{1}{\epsilon})$, quadratic min-cost flow
Smoothing Prox-Grad	$O(\frac{1}{\epsilon})$, $O(J)$	$O(\frac{1}{\epsilon})$, $O(J \log J)$	$O(\frac{1}{\epsilon})$, $O(\sum_{g \in \mathcal{G}} g)$	$O(\frac{1}{\epsilon})$, $O(\sum_{g \in \mathcal{G}} g \log g)$	$O(\frac{1}{\epsilon})$, $O(\sum_{g \in \mathcal{G}} g)$	$O(\frac{1}{\epsilon})$, $O(\sum_{g \in \mathcal{G}} g \log g)$

model, $\mathbf{y} = \mathbf{X}\boldsymbol{\beta} + \boldsymbol{\epsilon}$, where $\boldsymbol{\beta}$ is the vector of length J for regression coefficients and $\boldsymbol{\epsilon}$ is the vector of length N for noise distributed as $N(0, \sigma^2 I_{N \times N})$. The standard lasso (Tibshirani, 1996) obtains a sparse estimate of the coefficients by solving the following optimization problem:

$$\min_{\boldsymbol{\beta} \in \mathbb{R}^J} g(\boldsymbol{\beta}) + \lambda \|\boldsymbol{\beta}\|_1, \quad (1)$$

where $g(\boldsymbol{\beta}) \equiv \frac{1}{2} \|\mathbf{y} - \mathbf{X}\boldsymbol{\beta}\|_2^2$ is the squared-error loss, $\|\boldsymbol{\beta}\|_1 \equiv \sum_{j=1}^J |\beta_j|$ is the ℓ_1 -norm penalty that encourages the solutions to be sparse, and λ is the regularization parameter that controls the sparsity level.

While the standard lasso penalty does not assume any structure among the input variables, recently various extensions of the lasso penalty have been proposed that incorporate the prior knowledge on the structure over the input variables to estimate a joint sparsity pattern among related inputs. We broadly call the structured-sparsity-inducing penalty $\Omega(\boldsymbol{\beta})$ without assuming a specific form, and define the problem of estimating a structured-sparsity pattern in the coefficients as follows:

$$\min_{\boldsymbol{\beta} \in \mathbb{R}^J} f(\boldsymbol{\beta}) \equiv g(\boldsymbol{\beta}) + \Omega(\boldsymbol{\beta}) + \lambda \|\boldsymbol{\beta}\|_1. \quad (2)$$

As examples of such penalties, in this paper, we consider two broad categories of penalties $\Omega(\boldsymbol{\beta})$ based on two different types of functional forms, namely overlapping-group-lasso penalty based on the ℓ_1/ℓ_2 mixed-norm and graph-guided fusion penalty. As we discuss below, these two types of penalties cover a broad set of structured-sparsity-inducing penalties that have been introduced in the literature (Yuan and Lin, 2006; Jenatton et al., 2009; Kim and Xing, 2010; Zhao et al., 2009; Tibshirani and Saunders, 2005; Kim et al., 2009).

1. Overlapping-group-lasso Penalty

Assuming that the set of groups of inputs $\mathcal{G} = \{g_1, \dots, g_{|\mathcal{G}|}\}$ is defined as a subset of the power set of $\{1, \dots, J\}$, and is available as prior knowledge. Note that members

of \mathcal{G} (groups) are allowed to overlap. The overlapping-group-lasso penalty based on the ℓ_1/ℓ_2 mixed-norm (Jenatton et al., 2009) is defined as:

$$\Omega(\boldsymbol{\beta}) \equiv \gamma \sum_{g \in \mathcal{G}} w_g \|\boldsymbol{\beta}_g\|_2, \quad (3)$$

where $\boldsymbol{\beta}_g \in \mathbb{R}^{|g|}$ is the subvector of $\boldsymbol{\beta}$ for the inputs in group g ; w_g is the predefined weight for group g ; and $\|\cdot\|_2$ is the vector ℓ_2 -norm. We assume that each group has at least two variables since otherwise the penalty for that group can be incorporated into the ℓ_1 -norm in (2). The ℓ_1/ℓ_2 mixed-norm penalty $\Omega(\boldsymbol{\beta})$ plays the role of setting all of the coefficients within each group to zero or non-zero values. It is worthy to note that the ℓ_1/ℓ_∞ mixed-norm penalty can also achieve the similar grouping effect. Although our approach can also be used for the ℓ_1/ℓ_∞ as well, in this paper, we focus on the ℓ_1/ℓ_2 penalty and the comparison between the ℓ_1/ℓ_2 and the ℓ_1/ℓ_∞ is beyond the scope of the paper.

Most of the existing optimization methods developed for mixed-norm penalties can handle only a specific subclass of the general overlapping-group-lasso penalties. Most of these methods use the proximal gradient framework (Beck and Teboulle, 2009; Nesterov, 2007) and focus on the issue of how to *exactly* solve the proximal operator. For non-overlapping groups with the ℓ_1/ℓ_2 or ℓ_1/ℓ_∞ mixed-norms, the proximal operator can be solved via a simple projection (Liu et al., 2009; Duchi and Singer, 2009). A one-pass coordinate ascent method has been developed for tree-structured groups with the ℓ_1/ℓ_2 or ℓ_1/ℓ_∞ (Jenatton et al., 2010; Liu and Ye, 2010b), and quadratic min-cost network flow for arbitrary overlapping groups with the ℓ_1/ℓ_∞ (Mairal et al., 2010).

Table 1 summarizes the applicability, the convergence rate, and the per-iteration time complexity for the available first-order methods for different subclasses of group lasso penalties. More specifically, the first three rows adopts the proximal gradient framework and the first column of these rows gives the algorithms for solving the proximal operator and the corresponding references. Each entry contains the convergence rate and the per-iteration time complexity. For the sake of simplicity, in all of the entries, we omit the time for computing the gradient of the loss function which is needed for all the methods (i.e., $\nabla g(\boldsymbol{\beta})$ with $O(J^2)$). The per-iteration time complexity in the table may come from the computation of proximal operator or subgradient of the penalty. ‘‘N.A.’’ stands for ‘‘not applicable’’ or no guarantee in the convergence. For comparison, we show the same information of the proposed method in the last row of Table 1. Although our method is not the most ideal one for some of the special cases, our method along with FOBOS² (Duchi and Singer, 2009) are the only generic methods that can be applied to all subclasses of the penalties.

2. We note that in contrast to other proximal gradient methods which require the loss function (i.e. first part of the objective) to be smooth, FOBOS is a more general framework in that it allows the non-smoothness of the loss function. It performs the subgradient descent on the loss and solves the proximal operator associated with the penalty. If the loss function is smooth and the proximal operator can be solved exactly, it achieves $O(\frac{1}{\epsilon})$ convergence rate. Otherwise, if the proximal operator cannot be exactly solved, FOBOS reduces to the subgradient descent on the sum of the loss and the penalty with $O(\frac{1}{\epsilon^2})$ convergence rate.

As we can see from Table 1, for arbitrary overlaps with the ℓ_1/ℓ_∞ , although the method proposed in (Mairal et al., 2010) achieves $O(\frac{1}{\sqrt{\epsilon}})$ convergence rate, the per-iteration complexity could be high due to solving a quadratic min-cost network flow problem. From the worst-case analysis, the per-iteration time complexity for solving the network flow problem in (Mairal et al., 2010) is at least $O(|V||E|) = O((J + |\mathcal{G}|)(|\mathcal{G}| + J + \sum_{g \in \mathcal{G}} |g|))$, which is much higher than our method with $O(\sum_{g \in \mathcal{G}} |g| \log |g|)$. More importantly, for the case of arbitrary overlaps with the ℓ_1/ℓ_2 , our method has a superior convergence rate to all the other methods.

In addition to these methods, an active-set algorithm was proposed that applies to the *square* of the ℓ_1/ℓ_2 mixed-norm with overlapping groups (Jenatton et al., 2009). This method formulates each subproblem involving only the active variables either as an SOCP, which can be computationally expensive for a large active set, or as a jointly convex problem with auxiliary variables, which is then solved by an alternating gradient descent. The latter approach involves an expensive matrix inversion at each iteration and lacks the global convergence rate. Another method (Liu and Ye, 2010a) was proposed for overlapping group lasso which approximately solves the proximal operator. However, the convergence of such type of approach cannot be guaranteed, since the error introduced in each proximal operator will be accumulated over iterations. A primal-dual algorithm (Mosci et al., 2010) was proposed to solve a different formulation of group lasso problem in (Jacob et al., 2009).

2. Graph-guided Fusion Penalty

Let us assume the structure of J input variables is available as a graph G with a set of nodes $V = \{1, \dots, J\}$ and a set of edges E . Let $r_{ml} \in \mathbb{R}$ denote the weight of the edge $e = (m, l) \in E$, corresponding to the correlation between the two inputs for nodes m and l . Then, the graph-guided fusion penalty as defined below generalizes chain-structured fused-lasso penalty proposed by Tibshirani and Saunders (2005):

$$\Omega(\boldsymbol{\beta}) = \gamma \sum_{e=(m,l) \in E, m < l} \tau(r_{ml}) |\beta_m - \text{sign}(r_{ml})\beta_l|, \quad (4)$$

where $\tau(r)$ weights the fusion penalty for each edge $e = (m, l)$ such that β_m and β_l for highly correlated inputs with larger $|r_{ml}|$ receive a greater fusion effect. In this paper, we consider $\tau(r) = |r|$, but any monotonically increasing function of the absolute values of correlations can be used. The $\text{sign}(r_{ml})$ indicates that for two positively correlated nodes, the corresponding coefficients tend to be influence the output in the same direction, while for two negatively correlated nodes, the effects (β_m and β_l) take the opposite direction. Since this fusion effect is calibrated by the edge weight, the graph-guided fusion penalty in (4) encourages highly correlated inputs corresponding to a densely connected subnetwork in G to be jointly selected as relevant. We notice that if $r_{ml} = 1$ for all $e = (m, l)$, the penalty function in (4) reduces to:

$$\Omega(\boldsymbol{\beta}) = \gamma \sum_{e=(m,l) \in E, m < l} |\beta_m - \beta_l|. \quad (5)$$

The standard fused lasso penalty $\gamma \sum_{j=1}^{J-1} |\beta_{j+1} - \beta_j|$ is special case of (5), where the graph structure is confined to be a chain (Tibshirani and Saunders, 2005) and

the widely used fused signal approximator refers to the simple case where the design matrix \mathbf{X} is orthogonal.

For the graph-guided fusion penalty, when the structure is a simple chain, pathwise coordinate descent method (Friedman et al., 2007) can be applied. For the general graph structure, a first-order method that approximately solves the proximal operator was proposed (Liu et al., 2010). However, the convergence cannot be guaranteed due to the errors introduced in computing the proximal operator over iterations. Recently, a different algorithm has been proposed that reformulates the problem as a maximum flow problem (Hoeffling, 2009). This algorithm is limited in that it can not be applied to the case where the dimension is more than the sample size which is the typical setting for sparse regression problems. Another work for solving the graph-guided fused lasso in (Tibshirani and Taylor, 2010) also suffers from the same problem. In addition, all these work lack the theoretical analysis of the convergence.

3. Smoothing Proximal Gradient

In this section, we present the smoothing proximal gradient method. The main difficulty in optimizing (2) arises from the non-separability of β in the non-smooth penalty $\Omega(\beta)$. For both types of penalties, we show that using the dual norm, the non-separable structured-sparsity-inducing penalties $\Omega(\beta)$ can be formulated as $\Omega(\beta) = \max_{\alpha \in \mathcal{Q}} \alpha^T C \beta$. Based on that, we introduce a smooth approximation to $\Omega(\beta)$ such that its gradient can be easily calculated.

3.1 Reformulation of the Structured-sparsity-inducing Penalty

In this section, we show that despite the non-separability, by using the dual norm, both types of the structured-sparsity-inducing penalties in (3) and (4) can be decoupled once we reformulate them into the common form of a maximization problem over the auxiliary variables.

1. Overlapping-group-lasso Penalty

Since the dual norm of ℓ_2 -norm is also an ℓ_2 -norm, we can write $\|\beta_g\|_2$ as $\|\beta_g\|_2 = \max_{\|\alpha_g\|_2 \leq 1} \alpha_g^T \beta_g$, where $\alpha_g \in \mathbb{R}^{|g|}$ is the vector of auxiliary variables associated with β_g . Let $\alpha = [\alpha_{g_1}^T, \dots, \alpha_{g_{|G|}}^T]^T$. Then, α is a vector of length $\sum_{g \in G} |g|$ with domain $\mathcal{Q} \equiv \{\alpha \mid \|\alpha_g\|_2 \leq 1, \forall g \in \mathcal{G}\}$, where \mathcal{Q} is the Cartesian product of unit balls in Euclidean space and thus, a closed and convex set. We can rewrite the overlapping-group-lasso penalty in (3) as:

$$\Omega(\beta) = \gamma \sum_{g \in \mathcal{G}} w_g \max_{\|\alpha_g\|_2 \leq 1} \alpha_g^T \beta_g = \max_{\alpha \in \mathcal{Q}} \sum_{g \in \mathcal{G}} \gamma w_g \alpha_g^T \beta_g = \max_{\alpha \in \mathcal{Q}} \alpha^T C \beta, \quad (6)$$

where $C \in \mathbb{R}^{\sum_{g \in \mathcal{G}} |g| \times J}$ is a matrix defined as follows. The rows of C are indexed by all pairs of $(i, g) \in \{(i, g) \mid i \in g, i \in \{1, \dots, J\}\}$, the columns are indexed by $j \in \{1, \dots, J\}$, and each element of C is given as:

$$C_{(i,g),j} = \begin{cases} \gamma w_g & \text{if } i = j, \\ 0 & \text{otherwise.} \end{cases} \quad (7)$$

Note that C is a highly sparse matrix with only a single non-zero element in each row and $\sum_{g \in \mathcal{G}} |g|$ non-zero elements in the entire matrix, and hence, can be stored with only a small amount of memory during the optimization procedure.

2. Graph-guided Fusion Penalty

First, we rewrite the graph-guided fusion penalty in (4) as follows:

$$\gamma \sum_{e=(m,l) \in E, m < l} \tau(r_{ml}) |\beta_m - \text{sign}(r_{ml})\beta_l| \equiv \|C\beta\|_1,$$

where $C \in \mathbb{R}^{|E| \times J}$ is the edge-vertex incident matrix:

$$C_{e=(m,l),j} = \begin{cases} \gamma \cdot \tau(r_{ml}) & \text{if } j = m \\ -\gamma \cdot \text{sign}(r_{ml})\tau(r_{ml}) & \text{if } j = l \\ 0 & \text{otherwise.} \end{cases} \quad (8)$$

Again, we note that C is a highly sparse matrix with $2 \cdot |E|$ non-zero elements.

Since the dual norm of the ℓ_∞ -norm is the ℓ_1 -norm, we can further rewrite the graph-guided fusion penalty as:

$$\|C\beta\|_1 \equiv \max_{\|\alpha\|_\infty \leq 1} \alpha^T C\beta, \quad (9)$$

where $\alpha \in \mathcal{Q} = \{\alpha \mid \|\alpha\|_\infty \leq 1, \alpha \in \mathbb{R}^{|E|}\}$ is a vector of auxiliary variables associated with $\|C\beta\|_1$, and $\|\cdot\|_\infty$ is the ℓ_∞ -norm defined as the maximum absolute value of all entries in the vector.

Remark 1 *As a generalization of graph-guided fusion penalty, the proposed optimization method can be applied to the ℓ_1 -norm of any linear mapping of β (i.e., $\Omega(\beta) = \|C\beta\|_1$ for any given C).*

3.2 Smooth Approximation of Structured-sparsity-inducing Penalty

The common formulation of $\Omega(\beta)$ (i.e., $\Omega(\beta) = \max_{\alpha \in \mathcal{Q}} \alpha^T C\beta$) is still a non-smooth function of β , and this makes the optimization challenging. To tackle this problem, using the smoothing technique from (Nesterov, 2005), we construct a smooth approximation of $\Omega(\beta)$ as following:

$$f_\mu(\beta) = \max_{\alpha \in \mathcal{Q}} (\alpha^T C\beta - \mu d(\alpha)), \quad (10)$$

where μ is the positive smoothness parameter and $d(\alpha)$ is defined as $\frac{1}{2}\|\alpha\|_2^2$. The original penalty term can be viewed as $f_\mu(\beta)$ with $\mu = 0$. It is easy to see that $f_\mu(\beta)$ is a lower bound of $f_0(\beta)$. In order to bound the gap between $f_\mu(\beta)$ and $f_0(\beta)$, let $D = \max_{\alpha \in \mathcal{Q}} d(\alpha)$. In our problems, $D = |\mathcal{G}|/2$ for the overlapping-group-lasso penalty and $D = |E|/2$ for the graph-guided fusion penalty. Then, it is easy to verify that the maximum gap between $f_\mu(\beta)$ and $f_0(\beta)$ is μD :

$$f_0(\beta) - \mu D \leq f_\mu(\beta) \leq f_0(\beta).$$

From Theorem 1 as presented below, we know that $f_\mu(\beta)$ is a smooth function for any $\mu > 0$. Therefore, $f_\mu(\beta)$ can be viewed as a *smooth approximation* of $f_0(\beta)$ with the maximum gap

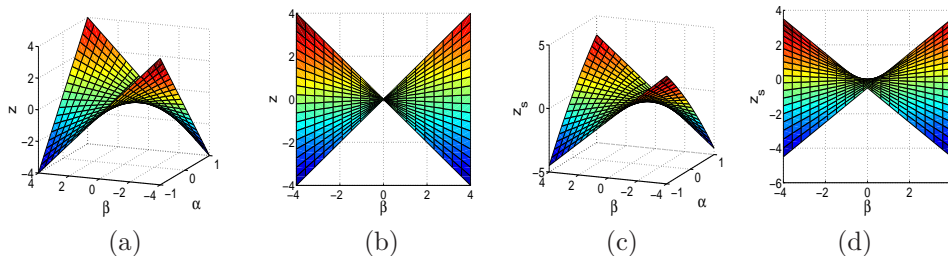


Figure 1: A geometric illustration of the smoothness of $f_\mu(\beta)$. (a) The 3-D plot of $z(\alpha, \beta)$, (b) the projection of (a) onto the β - z space, (c) the 3-D plot of $z_s(\alpha, \beta)$, and (d) the projection of (c) onto the β - z space.

of μD , and the μ controls the gap between $f_\mu(\beta)$ and $f_0(\beta)$. Given the desired accuracy ϵ , the convergence result in Section 3.4 suggests $\mu = \frac{\epsilon}{2D}$ to achieve the best convergence rate.

Now we present the key theorem (Nesterov, 2005) to show that $f_\mu(\beta)$ is smooth in β with a simple form of the gradient.

Theorem 2 *For any $\mu > 0$, $f_\mu(\beta)$ is a convex and continuously-differentiable function in β , and the gradient of $f_\mu(\beta)$ takes the following form:*

$$\nabla f_\mu(\beta) = C^T \alpha^*, \quad (11)$$

where α^* is the optimal solution to (10). Moreover, the gradient $\nabla f_\mu(\beta)$ is Lipschitz continuous with the Lipschitz constant $L_\mu = \frac{1}{\mu} \|C\|^2$, where $\|C\|$ is a special norm of C defined as $\|C\| \equiv \max_{\|\mathbf{v}\|_2 \leq 1} \|C\mathbf{v}\|_2$.

This theorem is given in (Nesterov, 2005) but without a detailed proof of smoothness and a derivation of the gradient. Just for the purpose of completeness, we show that by viewing $f_\mu(\beta)$ as the *Fenchel Conjugate* of $d(\cdot)$ at $\frac{C\beta}{\mu}$, the smoothness can be obtained by applying Theorem 26.3 in (Rockafellar, 1996). The gradient in (11) can be derived from the Danskin's Theorem (Bertsekas, 1999) and the Lipschitz constant is shown in (Nesterov, 2005). The details are discussed in the appendix.

To provide insights on why $f_\mu(\beta)$ is a smooth function as Theorem 1 suggests, in Figure 1, we show a geometric illustration for the case of one-dimensional parameter (i.e., $\beta \in \mathbb{R}$). For the sake of simplicity, we assume that μ and C are set to 1. First, we show geometrically that $f_0(\beta) = \max_{\alpha \in [-1, 1]} z(\alpha, \beta)$, where $z(\alpha, \beta) \equiv \alpha\beta$, is a non-smooth function. The three-dimensional plot for $z(\alpha, \beta)$ with α restricted to $[-1, 1]$ is shown in Figure 1(a). We project the surface in Figure 1(a) onto the β - z space as shown in Figure 1(b). For each β , the value of $f_0(\beta)$ is the highest point along the z -axis since we maximize over α in $[-1, 1]$. We can see that $f_0(\beta)$ is composed of two segments with a sharp point at $\beta = 0$. Now, we introduce the auxiliary function, and let $z_s(\alpha, \beta) \equiv \alpha\beta - \frac{1}{2}\alpha^2$ and $f_\mu(\beta) = \max_{\alpha \in [-1, 1]} z_s(\alpha, \beta)$. The three-dimensional plot for $z_s(\alpha, \beta)$ with α restricted to $[-1, 1]$ is shown in Figure 1(c). Similarly, we project the surface in Figure 1(c) onto the β - z_s space as shown in Figure 1(d). For fixed β , the value of $f_\mu(\beta)$ is the highest point along the z -axis. In Figure 1(d), we can see that $f_\mu(\beta)$ is composed of three parts: (i) a line with slope -1 when $\beta < 1$,

(ii) a line with slope 1 when $\beta > 1$, and (iii) a quadratic function when $-1 \leq \beta \leq 1$. By introducing an auxiliary quadratic function, we remove the sharp point at $\beta = 0$ and $f_\mu(\beta)$ becomes a smooth function.

To compute the $\nabla f_\mu(\beta)$ and L_μ , we need to know α^* and $\|C\|$. We present the closed-form equations for α^* and $\|C\|$ for the overlapping-group-lasso penalty and graph-guided fusion penalty in the following propositions and the proof is presented in the appendix.

1. Overlapping-group-lasso Penalty

Proposition 3 *Let α^* , which is composed of $\{\alpha_g^*\}_{g \in \mathcal{G}}$, be the optimal solution to (10) for overlapping-group-lasso penalty in (3). For any $g \in \mathcal{G}$,*

$$\alpha_g^* = S\left(\frac{\gamma w_g \beta_g}{\mu}\right),$$

where S is the projection operator which projects any vector \mathbf{u} to the ℓ_2 ball:

$$S(\mathbf{u}) = \begin{cases} \frac{\mathbf{u}}{\|\mathbf{u}\|_2} & \|\mathbf{u}\|_2 > 1, \\ \mathbf{u} & \|\mathbf{u}\|_2 \leq 1. \end{cases}$$

$$\|C\| = \gamma \max_{j \in \{1, \dots, J\}} \sqrt{\sum_{g \in \mathcal{G} \text{ s.t. } j \in g} (w_g)^2}.$$

2. Graph-guided Fusion Penalty

Proposition 4 *Let α^* be the optimal solution of (10) for graph-guided fusion penalty in (4). Then, we have:*

$$\alpha^* = S\left(\frac{C\beta}{\mu}\right),$$

where S is the shrinkage operator defined as follows:

$$S(x) = \begin{cases} x, & \text{if } -1 \leq x \leq 1 \\ 1, & \text{if } x > 1 \\ -1, & \text{if } x < -1. \end{cases}$$

For any vector α , $S(\alpha)$ is defined as applying S on each and every entry of α .

$\|C\|$ is upper-bounded by $\sqrt{2\gamma^2 \max_{j \in V} d_j}$, where

$$d_j = \sum_{e \in E \text{ s.t. } e \text{ incident on } j} (\tau(r_e))^2 \tag{12}$$

for $j \in V$ in graph G , and this bound is tight. Note that when $\tau(r_e) = 1$ for all $e \in E$, d_j is simply the degree of the node j .

3.3 Smoothing Proximal Gradient Descent

Given the smooth approximation of the non-smooth structured-sparsity-inducing penalties as presented in the previous section, now, we apply the fast iterative shrinkage-thresholding algorithm (FISTA) (Beck and Teboulle, 2009), using the gradient information in Theorem 2. We substitute the penalty term $\Omega(\boldsymbol{\beta})$ in (2) with its smooth approximation $f_\mu(\boldsymbol{\beta})$ to obtain the following optimization problem:

$$\min_{\boldsymbol{\beta}} \tilde{f}(\boldsymbol{\beta}) \equiv g(\boldsymbol{\beta}) + f_\mu(\boldsymbol{\beta}) + \lambda \|\boldsymbol{\beta}\|_1. \quad (13)$$

Let

$$h(\boldsymbol{\beta}) = g(\boldsymbol{\beta}) + f_\mu(\boldsymbol{\beta}) = \frac{1}{2} \|\mathbf{y} - \mathbf{X}\boldsymbol{\beta}\|_2^2 + f_\mu(\boldsymbol{\beta}).$$

According to Theorem 2, the gradient of $h(\boldsymbol{\beta})$ is given as:

$$\nabla h(\boldsymbol{\beta}) = \mathbf{X}^T(\mathbf{X}\boldsymbol{\beta} - \mathbf{y}) + C^T \boldsymbol{\alpha}^*. \quad (14)$$

Moreover, $\nabla h(\boldsymbol{\beta})$ is Lipschitz-continuous with the Lipschitz constant:

$$L = \lambda_{\max}(\mathbf{X}^T \mathbf{X}) + L_\mu = \lambda_{\max}(\mathbf{X}^T \mathbf{X}) + \frac{\|C\|^2}{\mu}, \quad (15)$$

where $\lambda_{\max}(\mathbf{X}^T \mathbf{X})$ is the largest eigenvalue of $(\mathbf{X}^T \mathbf{X})$.

Since $f(\boldsymbol{\beta})$ only involves a very simple non-smooth part (i.e., the ℓ_1 -norm penalty), we can adopt FISTA (Beck and Teboulle, 2009) to minimize $\tilde{f}(\boldsymbol{\beta})$ as shown in Algorithm 1. Algorithm 1 alternates between the sequences $\{w^t\}$ and $\{\boldsymbol{\beta}^t\}$ and $\theta_t = \frac{2}{t+2}$ can be viewed as a special ‘‘step-size’’, which determines the relationship between $\{w^t\}$ and $\{\boldsymbol{\beta}^t\}$ as in Step 4 of Algorithm 1. As shown in (Beck and Teboulle, 2009), such a way of setting θ_t leads to Lemma 1 in Appendix, which further guarantees the convergence result in Theorem 7.

Rewriting (16), we can easily see that it is the proximal operator associated with the ℓ_1 -norm :

$$\boldsymbol{\beta}^{t+1} = \arg \min_{\boldsymbol{\beta}} \frac{1}{2} \|\boldsymbol{\beta} - (\mathbf{w}^t - \frac{1}{L} \nabla h(\mathbf{w}^t))\|_2^2 + \frac{\lambda}{L} \|\boldsymbol{\beta}\|_1.$$

Let $\mathbf{v} = (\mathbf{w}^t - \frac{1}{L} \nabla h(\mathbf{w}^t))$, the closed-form solution for $\boldsymbol{\beta}^{t+1}$ can be obtained by soft-thresholding (Friedman et al., 2007) as presented in the next proposition.

Proposition 5 *The closed-form solution of*

$$\min_{\boldsymbol{\beta}} \frac{1}{2} \|\boldsymbol{\beta} - \mathbf{v}\|_2^2 + \frac{\lambda}{L} \|\boldsymbol{\beta}\|_1$$

can be obtained by the soft-thresholding operation:

$$\beta_j = \text{sign}(v_j) \max(0, |v_j| - \frac{\lambda}{L}), \quad j = 1, \dots, J. \quad (17)$$

A notable advantage of utilizing the proximal operator associated with the ℓ_1 -norm penalty as in Step 2 of Algorithm 1 is that it can provide us with the sparse solutions, where the coefficients for irrelevant inputs are set *exactly* to zero, due to the soft-thresholding operation in (17). At convergence, the values of $\boldsymbol{\beta}$ for the irrelevant groups in the group-lasso penalty and edges in the graph-guided fusion penalty will become sufficiently close to zeros, and the soft-thresholding operation will truncate them exactly to zeros.

Algorithm 1 Smoothing Proximal Gradient Method for Structured Sparse Regression

Input: \mathbf{X} , \mathbf{y} , C , β^0 , desired accuracy ϵ .

Initialization: set $\mu = \frac{\epsilon}{2D}$, $\theta_0 = 1$, $\mathbf{w}^0 = \beta^0$.

Iterate For $t = 0, 1, 2, \dots$, until convergence of β^t :

1. Compute $\nabla h(\mathbf{w}^t)$ according to (14).
2. Solve the proximal operator associated with the ℓ_1 -norm:

$$\beta^{t+1} = \arg \min_{\beta} h(\mathbf{w}^t) + \langle \beta - \mathbf{w}^t, \nabla h(\mathbf{w}^t) \rangle + \lambda \|\beta\|_1 + \frac{L}{2} \|\beta - \mathbf{w}^t\|_2^2 \quad (16)$$

3. Set $\theta_{t+1} = \frac{2}{t+3}$.
4. Set $\mathbf{w}^{t+1} = \beta^{t+1} + \frac{1-\theta_t}{\theta_t} \theta_{t+1} (\beta^{t+1} - \beta^t)$.

Output: $\hat{\beta} = \beta^{t+1}$.

Remark 6 Algorithm 1 is a general approach that can be applied to any smooth convex loss (e.g. logistic loss). with the structured-sparsity-inducing penalty $\Omega(\beta)$ that can be re-written in the form of $\max_{\alpha} \alpha^T C \beta$.

3.4 Convergence Rate and Time Complexity

Although we optimize the approximation function $\tilde{f}(\beta)$ rather than optimizing $f(\beta)$ directly, it can be proven that the $\hat{\beta}$ obtained from Algorithm 1 is sufficiently close to the optimal solution β^* to the original optimization problem in (2). We present the convergence rate of Algorithm 1 in the next theorem.

Theorem 7 Let β^* be the optimal solution to (2) and β^t be the approximate solution at the t -th iteration in Algorithm 1. If we require $f(\beta^t) - f(\beta^*) \leq \epsilon$ and set $\mu = \frac{\epsilon}{2D}$, then, the number of iterations t is upper-bounded by

$$\sqrt{\frac{4\|\beta^* - \beta^0\|_2^2}{\epsilon} \left(\lambda_{\max}(\mathbf{X}^T \mathbf{X}) + \frac{2D\|C\|^2}{\epsilon} \right)}. \quad (18)$$

A bound similar to (18) has been shown in (Lan et al., 2011) where the smoothing technique is combined with a different first-order algorithm instead of FISTA. The key idea behind the proof of this theorem is to decompose $f(\beta^t) - f(\beta^*)$ into three parts: (i) $f(\beta^t) - \tilde{f}(\beta^t)$, (ii) $\tilde{f}(\beta^t) - \tilde{f}(\beta^*)$, and (iii) $\tilde{f}(\beta^*) - f(\beta^*)$. (i) and (iii) can be bounded by the gap of the approximation μD . (ii) only involves the function f and can be upper bounded by $O(\frac{1}{t^2})$ as shown in (Beck and Teboulle, 2009) by balancing these three terms. The details of the proof are presented in Appendix. We obtain (18). According to Theorem 7, Algorithm 1 converges in $O(\frac{\sqrt{2D}}{\epsilon})$ iterations, which is much faster than the subgradient method with the convergence rate of $O(\frac{1}{\epsilon^2})$. Note that the convergence rate depends on D through the term $\sqrt{2D}$, and the D depends on the problem size.

Table 2: Comparison of Per-iteration Time Complexity

	Overlapping Group Lasso	Graph-guided Fused Lasso
Smoothing Proximal Gradient	$O(J^2 + \sum_{g \in \mathcal{G}} g)$	$O(J^2 + E)$
IPM for SOCP	$O\left((J + \mathcal{G})^2(N + \sum_{g \in \mathcal{G}} g)\right)$	$O\left((J + E)^2(N + J + E)\right)$

As for the time complexity, assuming that we can pre-compute and store $\mathbf{X}^T \mathbf{X}$ and $\mathbf{X}^T \mathbf{y}$ with the time complexity of $O(J^2 N)$, the main computational cost in each iteration comes from calculating the gradient $\nabla h(\mathbf{w}_t)$. As we discussed in the Section 2, the existing methods for solving (2) with the ℓ_1/ℓ_2 mixed-norm based overlapping-group-lasso penalty include FOBOS (Duchi and Singer, 2009) (or subgradient descent) and IPM for SOCP. The first approach has the same per-iteration time complexity as our method but with $O(\frac{1}{\epsilon^2})$ convergence rate. For IPM for SOCP, although it converges in fewer iterations (i.e., $\log(\frac{1}{\epsilon})$), its per-iteration complexity is higher by orders of magnitude than ours as shown in Table 2. Therefore, the smoothing proximal gradient method is much more efficient and scalable for large-scale problems. In addition to time complexity, each IPM iteration of SOCP requires significantly more memory to store the Newton linear system.

Remark 8 *If we can pre-compute and store $\mathbf{X}^T \mathbf{X}$, the per-iteration time complexity of our method is independent of sample size N as shown in Table 2. If J is very large, $\mathbf{X}^T \mathbf{X}$ may not fit into memory. In such a case, we compute $\mathbf{X}^T(\mathbf{X}\mathbf{w}^t)$ for each iteration; and the per-iteration time complexity will increase by a factor of N but still less than that for IPM for SOCP. For the logistic loss, the per-iteration complexity is also linear in N .*

3.5 Summary and Discussions

The insight of our work was drawn from two lines of earlier works. The first one is the proximal gradient methods (e.g., Nesterov’s composite gradient method (Nesterov, 2007), FISTA (Beck and Teboulle, 2009)). They have been widely adopted to solve optimization problems with a convex loss and a relatively simple non-smooth penalty, and achieve $O(\frac{1}{\sqrt{\epsilon}})$ convergence rate. However, the complex structure of the non-separable penalties considered in this paper makes it intractable to solve the proximal operator exactly. This is the challenge that we circumvent via smoothing.

The idea of smoothing the non-smooth function was first discussed in (Nesterov, 2005). The algorithm presented in (Nesterov, 2005) only works for smooth problems so that it has to smooth out the entire non-smooth penalty (including the ℓ_1 -norm). However, it is precisely the *non-smoothness* of the penalty that leads to exact zeros in optimal solutions. Therefore, although widely adopted in optimization field, this approach cannot yield exact zero solution and leads the problem of where to truncate the solution to zero. Moreover, the algorithm in (Nesterov, 2005) requires the condition that β is bounded and that the number of iterations is pre-defined, which are impractical for real applications. Instead, our approach combines the smoothing idea with the proximal gradient method and hence leads to the exact sparse solutions.

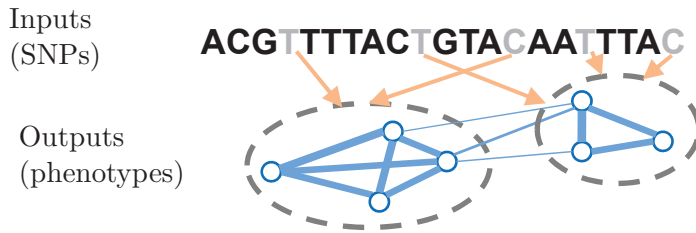


Figure 2: Illustration of the multivariate regression with graph structure on outputs.

As for the convergence rate, the gap between $O(\frac{1}{\epsilon})$ and the optimal rate $O(\frac{1}{\sqrt{\epsilon}})$ is due to the approximation of the structured-sparsity-inducing penalty. It is possible to show that if $\mathbf{X}^T \mathbf{X}$ is a positive definite (PD) matrix, $O(\frac{1}{\sqrt{\epsilon}})$ can be achieved by a variant of excessive gap method (Nesterov, 2003). However, such a rate can not be easily obtained for sparse regression problems where $J > N$ (i.e., $\mathbf{X}^T \mathbf{X}$ is not PD). For some special cases as discussed in Section 2, such as tree-structured or the ℓ_1/ℓ_∞ mixed-norm based overlapping groups, $O(\frac{1}{\sqrt{\epsilon}})$ can be achieved at the expense of more computation time for solving the proximal operator. It remains an open question whether we can further boost the generally-applicable smoothing proximal gradient method to achieve $O(\frac{1}{\sqrt{\epsilon}})$.

4. Extensions for Multivariate Regression

The structured-sparsity-inducing penalties as discussed in the previous section can be similarly used in the multivariate regression setting (Kim and Xing, 2010; Kim et al., 2009) where the prior structural information is available for the outputs. For example, in genetic association analysis, where the goal is to discover few genetic variants or single nucleotide polymorphisms (SNPs) out of millions of SNPs (inputs) that influence phenotypes (outputs) such as gene expression measurements, the correlation structure of phenotypes can be naturally represented as a graph, which can be used to guide the selection of SNPs as shown in Figure 2. Then, the graph-guided fusion penalty can be used to identify SNPs that are relevant jointly to multiple related phenotypes.

While in the multivariate regression problems, we encounter the same difficulties of optimizing with non-smooth and non-separable penalties as in the previous section, the smoothing proximal gradient method can be extended to this problem in a straightforward manner. Due to the importance of applications, in this section, we briefly discuss how our method can be applied to the multivariate regression with structured-sparsity-inducing penalties.

4.1 Multivariate Linear Regression Regularized by Structured-sparsity-inducing Penalties

Let $\mathbf{X} \in \mathbb{R}^{N \times J}$ denote the matrix of input data for J inputs and $\mathbf{Y} \in \mathbb{R}^{N \times K}$ denote the matrix of output data for K outputs over N samples. We assume a linear regression model for each of the k -th output: $\mathbf{y}_k = \mathbf{X} \boldsymbol{\beta}_k + \boldsymbol{\epsilon}_k$, $\forall k = 1, \dots, K$, where $\boldsymbol{\beta}_k = [\beta_{1k}, \dots, \beta_{Jk}]^T$ is the regression coefficient vector for the k -th output and $\boldsymbol{\epsilon}_k$ is Gaussian noise. Let $\mathbf{B} = [\boldsymbol{\beta}_1, \dots, \boldsymbol{\beta}_K] \in \mathbb{R}^{J \times K}$ be the matrix of regression coefficients for all of the K outputs. Then,

the multivariate structured sparse regression problem can be naturally formulated as the following optimization problem:

$$\min_{\mathbf{B} \in \mathbb{R}^{J \times K}} f(\mathbf{B}) \equiv \frac{1}{2} \|\mathbf{Y} - \mathbf{X}\mathbf{B}\|_F^2 + \Omega(\mathbf{B}) + \lambda \|\mathbf{B}\|_1, \quad (19)$$

where $\|\cdot\|_F$ denotes the matrix Frobenius norm, $\|\cdot\|_1$ denotes the matrix entry-wise ℓ_1 norm, and $\Omega(\mathbf{B})$ is a structured-sparsity-inducing penalty with the structure over outputs.

1. **Overlapping-group-lasso Penalty in Multivariate Regression:** We define the overlapping-group-lasso penalty for the in multivariate regression as follows:

$$\Omega(\mathbf{B}) \equiv \gamma \sum_{j=1}^J \sum_{g \in \mathcal{G}} w_g \|\beta_{jg}\|_2, \quad (20)$$

where $\mathcal{G} = \{g_1, \dots, g_{|\mathcal{G}|}\}$ is a subset of the power set of $\{1, \dots, K\}$ and β_{jg} is the vector of regression coefficients $\{\beta_{jk}, k \in g\}$. Both ℓ_1/ℓ_2 mixed-norm penalty for multivariate regression (Obozinski et al., 2009) and tree-guided group-lasso penalty (Kim and Xing, 2010) are special cases of (20).

2. **Graph-guided Fusion Penalty in Multivariate Regression:** Assuming the graph structure over the K outputs is given as G with a set of nodes $V = \{1, \dots, K\}$ and a set of edges E , the graph-guided fusion penalty for multivariate regression is given as:

$$\Omega(\mathbf{B}) = \gamma \sum_{e=(m,l) \in E} \tau(r_{ml}) \sum_{j=1}^J |\beta_{jm} - \text{sign}(r_{ml})\beta_{jl}|. \quad (21)$$

4.2 Smoothing Proximal Gradient Descent

Using the similar techniques in Section 3.1, $\Omega(\mathbf{B})$ can be reformulated as:

$$\Omega(\mathbf{B}) = \max_{\mathbf{A} \in \mathcal{Q}} \langle C\mathbf{B}^T, \mathbf{A} \rangle, \quad (22)$$

where $\langle \mathbf{U}, \mathbf{V} \rangle \equiv \text{Tr}(\mathbf{U}^T \mathbf{V})$ denotes a matrix inner product. C is constructed in the similar way as in (7) or (8) just by replacing the index of the input variables with the output variables, and \mathbf{A} is the matrix of auxiliary variables.

Then we introduce the smooth approximation of (22):

$$f_\mu(\mathbf{B}) = \max_{\mathbf{A} \in \mathcal{Q}} (\langle C\mathbf{B}^T, \mathbf{A} \rangle - \mu d(\mathbf{A})), \quad (23)$$

where $d(\mathbf{A}) \equiv \frac{1}{2} \|\mathbf{A}\|_F^2$. Following a proof strategy similar to that in Theorem 2, we can show that $f_\mu(\mathbf{B})$ is convex and smooth with gradient $\nabla f_\mu(\mathbf{B}) = (\mathbf{A}^*)^T C$, where \mathbf{A}^* is the optimal solution to (23). The closed-form solution of \mathbf{A}^* and the Lipschitz constant for $\nabla f_\mu(\mathbf{B})$ can be derived in the same way.

By substituting $\Omega(\mathbf{B})$ in (19) with $f_\mu(\mathbf{B})$, we can adopt Algorithm 1 to solve (19) with convergence rate of $O(\frac{1}{\epsilon})$. The per-iteration time complexity of our method is $O(J^2 K + J \sum_{g \in \mathcal{G}} |g|)$ for overlapping group lasso and $O(J^2 K + J|E|)$ for graph-guided fused lasso.

5. Experiment

In this section, we evaluate the scalability and efficiency of the smoothing proximal gradient method (Prox-Grad) and apply Prox-Grad on overlapping group lasso to a real genetic dataset.

For overlapping group lasso, we compare the Prox-Grad with the FOBOS (Duchi and Singer, 2009) and IPM for SOCP.³ For graph-guided fused lasso, we compare the running time of Prox-Grad with that of the FOBOS (Duchi and Singer, 2009) and IPM for QP.⁴ Note that for FOBOS, we set the “loss function” to be $l(\boldsymbol{\beta}) = g(\boldsymbol{\beta}) + \Omega(\boldsymbol{\beta})$ and the penalty to $\lambda\|\boldsymbol{\beta}\|_1$. As discussed in Section 2, for the non-smooth $l(\boldsymbol{\beta})$, FOBOS achieves $O\left(\frac{1}{\epsilon^2}\right)$ convergence rate, which is slower than Prox-Grad.

All experiments are performed on a standard PC with 4GB RAM and the software is written in MATLAB. The main difficulty in comparisons is a fair stopping criterion. Unlike IPM, Prox-Grad and FOBOS do not generate a dual solution, and therefore, it is not possible to compute a primal-dual gap, which is the traditional stopping criterion for IPM. Here, we adopt a widely used approach for comparing different methods in optimization literature. Since it is well known that IPM usually gives more accurate (i.e., lower) objective, we set the objective obtained from IPM as the optimal objective value and stop the first-order methods when the objective is below 1.001 times the optimal objective value. For large datasets for which IPM cannot be applied, we stop the first-order methods when the relative change in the objective is below 10^{-6} . In addition, we set the maximum iterations to be 20,000.

In simulation data, we constrain the regularization parameters such that $\lambda = \gamma$ and we assume that for each group g , $w_g = 1$. As for the smoothing parameter μ , μ is set to $\frac{\epsilon}{2D}$ according to Theorem 7, where D is determined by the problem size. It is natural that for large-scale problems with large D , a larger ϵ can be adopted without affecting the recovery quality significantly. Therefore, instead of setting ϵ , we directly set $\mu = 10^{-4}$, which provided us reasonably good approximation accuracies for different scales of problems based on our experience for a range of μ in simulations. As for FOBOS, we set the stepsize rate to $\frac{c}{\sqrt{t}}$ as suggested in (Duchi and Singer, 2009), where c is set to $\frac{0.1}{\sqrt{NJ}}$ for univariate regression and $\frac{0.1}{\sqrt{NJK}}$ for multivariate regression.⁵

5.1 Simulation Study: Overlapping Group Lasso

We simulate data for a univariate linear regression model with the overlapping group structure as described below. Assuming that the inputs are ordered, we define a sequence of groups of 100 adjacent inputs with an overlap of 10 variables between two successive groups so that $\mathcal{G} = \{\{1, \dots, 100\}, \{91, \dots, 190\}, \dots, \{J - 99, \dots, J\}\}$ with $J = 90|\mathcal{G}| + 10$. We set $\beta_j = (-1)^j \exp(-(j-1)/100)$ for $1 \leq j \leq J$. We sample each element of \mathbf{X} from *i.i.d.* Gaussian distribution, and generate the output data from $\mathbf{y} = \mathbf{X}\boldsymbol{\beta} + \boldsymbol{\epsilon}$, where $\boldsymbol{\epsilon} \sim N(0, I_{N \times N})$.

-
3. We use the state-of-the-art MATLAB package SDPT3 (Tütüncü et al., 2003) for SOCP.
 4. We use the commercial package MOSEK (MOS) for QP. Graph-guided fused lasso can also be solved by SOCP but it is less efficient than QP.
 5. It is known that, empirically, a large c may lead to the failure of the convergence but a smaller value may make the optimization slow. According to our own experience with a range of values for c , such a way of setting c guarantees the convergence for all different scales of the problems studied in our experiment and provides us reasonably good empirical convergence speed.

Table 3: Comparisons of different optimization methods on the overlapping group lasso

$ \mathcal{G} = 10$ ($J = 910$)		$N=1,000$		$N=5,000$		$N=10,000$	
		CPU (s)	Obj.	CPU (s)	Obj.	CPU (s)	Obj.
$\gamma = 2$	SOCP	103.71	266.68	493.08	917.13	3777.46	1765.52
	FOBOS	27.12	266.95	1.71	918.02	1.48	1765.61
	Prox-Grad	0.87	266.95	0.71	917.46	1.28	1765.69
$\gamma = 0.5$	SOCP	106.02	83.30	510.56	745.10	3585.77	1596.42
	FOBOS	32.44	82.99	4.98	745.79	4.65	1597.53
	Prox-Grad	0.42	83.39	0.41	745.10	0.69	1596.45
$ \mathcal{G} = 50$ ($J = 4510$)		$N=1,000$		$N=5,000$		$N=10,000$	
		CPU (s)	Obj.	CPU (s)	Obj.	CPU (s)	Obj.
$\gamma = 10$	SOCP	4144.20	1089.01	-	-	-	-
	FOBOS	476.91	1191.05	394.75	1533.31	79.82	2263.49
	Prox-Grad	56.35	1089.05	77.61	1533.32	78.90	2263.60
$\gamma = 2.5$	SOCP	3746.43	277.91	-	-	-	-
	FOBOS	478.62	286.33	867.94	559.25	183.72	1266.73
	Prox-Grad	33.09	277.94	30.13	504.34	26.74	1266.72
$ \mathcal{G} = 100$ ($J = 9010$)		$N=1,000$		$N=5,000$		$N=10,000$	
		CPU (s)	Obj.	CPU (s)	Obj.	CPU (s)	Obj.
$\gamma = 20$	FOBOS	1336.72	2090.81	2261.36	3132.13	1091.20	3278.20
	Prox-Grad	234.71	2090.79	225.28	2692.98	368.52	3278.22
$\gamma = 5$	FOBOS	1689.69	564.21	2287.11	1302.55	3342.61	1185.66
	Prox-Grad	169.61	541.61	192.92	736.56	176.72	1114.93

To demonstrate the efficiency and scalability of Prox-Grad, we vary J , N and γ and report the total CPU time in seconds and the objective value in Table 3. The regularization parameter γ is set to either $|\mathcal{G}|/5$ or $|\mathcal{G}|/20$. As we can see from Table 3, firstly, both Prox-Grad and FOBOS are more efficient and scalable by orders of magnitude than IPM for SOCP. For larger J and N , we are unable to collect the results of SOCP. Secondly, Prox-Grad is more efficient than FOBOS for almost all different scales of the problems.⁶ Thirdly, for Prox-Grad, a smaller γ leads to faster convergence. This result is consistent with Theorem 7 which shows that the number of iterations is linear in γ through the term $\|C\|$. Moreover, we notice that a larger N may not increase the computational time for

6. In some entries in Table 3, the Obj. from FOBOS is much larger than other methods. This is because that FOBOS has reached the maximum number of iterations before convergence.

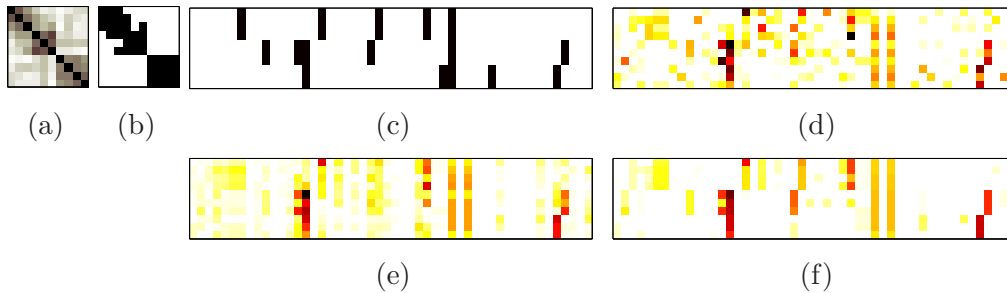


Figure 3: Regression coefficients estimated by different methods based on a single simulated dataset. $b = 0.8$ and threshold $\rho = 0.3$ for the output correlation graph are used. Red pixels indicate large values. (a) The correlation coefficient matrix of phenotypes, (b) the edges of the phenotype correlation graph obtained at threshold 0.3 are shown as black pixels, (c) the true regression coefficients used in simulation. Absolute values of the estimated regression coefficients are shown for (d) lasso, (e) ℓ_1/ℓ_2 regularized multivariate regression, (f) GFlasso. Rows correspond to outputs and columns to inputs.

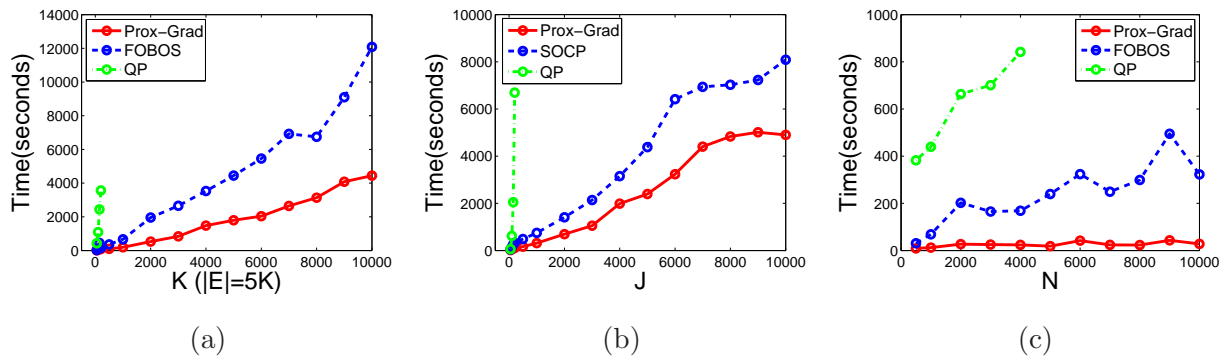


Figure 4: Comparisons of Prox-Grad, FOBOS and QP. (a) Vary K from 50 to 10,000, fixing $N = 500, J = 100$; (b) Vary J from 50 to 10,000, fixing $N = 1000, K = 50$; and (c) Vary N from 500 to 10000, fixing $J = 100, K = 50$.

Prox-Grad. This is also consistent with the time complexity analysis, which shows that for linear regression, the per-iteration time complexity is independent of N .

5.2 Simulation Study: Multivariate Graph-guided Fused Lasso

We simulate data using the following scenario analogous to the problem of genetic association mapping, where we are interested in identifying a small number of genetic variations (inputs) that influence the phenotypes (outputs). We use $K = 10, J = 30$ and $N = 100$. To simulate the input data, we use the genotypes of the 60 individuals from the parents of the HapMap CEU panel (The International HapMap Consortium, 2005), and generate genotypes for additional 40 individuals by randomly mating the original 60 individuals. We generate the regression coefficients β_k 's such that the outputs y_k 's are correlated with a block-like structure in the correlation matrix. We first choose input-output pairs with

non-zero regression coefficients as we describe below. We assume three groups of correlated output variables of sizes 3, 3, and 4. We randomly select inputs that are relevant jointly among the outputs within each group, and select additional inputs relevant across multiple groups to model the situation of a higher-level correlation structure across two subgraphs as in Figure 3(a). Given the sparsity pattern of \mathbf{B} , we set all non-zero β_{ij} to a constant $b = 0.8$ to construct the true coefficient matrix \mathbf{B} . Then, we simulate output data based on the linear regression model with noise distributed as standard Gaussian, using the simulated genotypes as inputs. We threshold the output correlation matrix in Figure 3(a) at $\rho = 0.3$ to obtain the graph in Figure 3(b), and use this graph as prior structural information for graph-guided fused lasso. As an illustrative example, the estimated regression coefficients from different methods are shown in Figures 3(d)–(f). While the results of lasso and ℓ_1/ℓ_2 -regularized multi-task regression in Figures 3(d) and (e) contain many false positives, the results from graph-guided fused lasso in Figure 3(f) show fewer false positives and reveal clear block structures. Thus, graph-guided fused lasso outperforms the other methods.

To compare Prox-Grad with FOBOS and IPM for QP, we vary K , J , N , and present the computation time in seconds in Figures 4(a)–(c), respectively. We select the regularization parameter γ using the separated validation dataset, and report the CPU time for GFlasso with the selected γ . The input, output and true regression coefficient \mathbf{B} are generated in the way similar as above. More precisely, we assume that each group of correlated output variables is of size 10. For each group of the outputs, We randomly select 10% of the input variables as relevant. In addition, we randomly select 5% of the input variables as relevant to every two consecutive groups of outputs and 1% of the input variables as relevant to every three consecutive groups. We set the ρ for each dataset so that the number of edges is 5 times the number of the nodes (i.e. $|E| = 5K$). Figure 4 shows that Prox-Grad is substantially more efficient and can scale up to very high-dimensional and large-scale datasets. Moreover, we notice that the increase of N almost does not affect the computation time of Prox-Grad, which is consistent with the complexity analysis in Section 3.4.

5.3 Real Data: Pathway Analysis of Breast Cancer Data

In this section, we apply the Prox-Grad with the overlapping-group-lasso penalty to a real-world dataset collected from breast cancer tumors (van de Vijver et al., 2002; Jacob et al., 2009) and solve it by the smoothing proximal gradient method. The data are given as gene expression measurements for 8,141 genes in 296 breast-cancer tumors (78 metastatic and 217 non-metastatic), and the task is to select a small amount of the most relevant genes that gives the best prediction performance.

Thus, a powerful way of discovering genes involved in a tumor growth is to consider groups of interacting genes in each pathway rather than individual genes independently (Ma and Kosorok, 2010). The overlapping-group-lasso penalty provides us with a natural way to incorporate these known pathway information into the biological analysis, where each group consists of the genes in each pathway. This approach can allow us to find pathway-level gene groups of significance that can distinguish the two tumor types. In our analysis of the breast cancer data, we cluster the genes using the canonical pathways from the Molecular Signatures Database (Subramanian et al., 2005), and construct the overlapping-group-lasso penalty using the pathway-based clusters as groups. Many of the groups overlap because

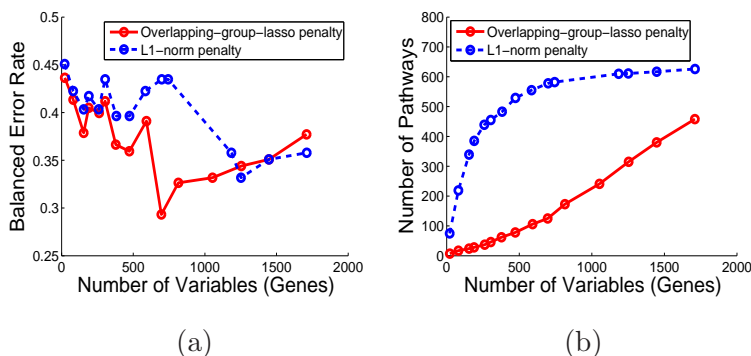


Figure 5: Results from the analysis of breast cancer dataset. (a) Balanced error rate for varying the number of selected genes, and (b) the number of pathways for varying the number of selected genes.

genes can participate in multiple pathways. Overall, we obtain 637 pathways over 3,510 genes, with each pathway containing 23.47 genes on average and each gene appearing in four pathways on average. Then, we set up the optimization problem of minimizing the logistic loss with the overlapping-group-lasso penalty to classify the tumor types based on the gene expression levels, and solve it with the Prox-Grad method.

Since the number of positive and negative samples are imbalanced, we adopt the balanced error rate defined as the average error rate of the two classes.⁷ We split the data into the training and testing sets with the ratio of 2:1, and vary the $\lambda = \gamma$ from large to small to obtain the full regularization path.

In Figure 5, we compare the results from fitting the logistic regression with the overlapping-group-lasso penalty and the model with the ℓ_1 -norm penalty. Figure 5(a) shows the balanced error rates for the different numbers of selected genes along the regularization path. As we can see, the balanced error rate for the model with the overlapping-group-lasso penalty is lower than the one with the ℓ_1 -norm, especially when the number of selected genes is between 500 to 1000. The model with the overlapping-group-lasso penalty achieves the best error rate of 29.23% when 696 genes are selected, and these 696 genes belong to 125 different pathways. In Figure 5(b), for the different numbers of selected genes, we show the number of pathways to which the selected genes belong. From Figure 5(b), we see that when the group structure information is incorporated, fewer pathways are selected. This indicates that regression with the overlapping-group-lasso penalty selects the genes at the pathway level as a functionally coherent groups, leading to an easy interpretation for functional analysis. On the other hand, the genes selected via the ℓ_1 -norm penalty are scattered across many pathways as genes are considered independently for selection. The total computational time for computing the whole regularization path with 20 different values for the regularization parameters is 331 seconds for the overlapping group lasso.

We perform a functional enrichment analysis on the selected pathways, using the functional annotation tool (Huang et al., 2009), and verify that the selected pathways are sig-

7. See <http://www.modelselect.inf.ethz.ch/evaluation.php> for more details

nificant in their relevance to the breast-cancer tumor types. For example, in a highly sparse model obtained with the group-lasso penalty at the very left end of Figure 5(b), the selected gene markers belong to only seven pathways, and many of these pathways appear to be reasonable candidates for an involvement in breast cancer. For instance, all proteins in one of the selected pathways are involved in the activity of *proteases* whose function is to degrade unnecessary or damaged proteins through a chemical reaction that breaks peptide bonds. One of the most important malignant properties of cancer involves the uncontrolled growth of a group of cells, and *protease inhibitors*, which degrade misfolded proteins, have been extensively studied in the treatment of cancer. Another interesting pathway selected by overlapping group lasso is known for its involvement in *nicotinate and nicotinamide metabolism*. This pathway has been confirmed as a marker for breast cancer in previous studies (Ma and Kosorok, 2010). In particular, the gene *ENPP1* (ectonucleotide pyrophosphatase/phosphodiesterase 1) in this pathway has been found to be overly expressed in breast tumors (Abate et al., 2005). Other selected pathways include the one related to ribosomes and another related to DNA polymerase, which are critical in the process of generating proteins from DNA and relevant to the property of uncontrolled growth in cancer cells.

We also examine the number of selected pathways that gives the lowest error rate in Figure 5. At the error rate of 29.23%, 125 pathways (696 genes) are selected. It is interesting to notice that among these 125 pathways, one is closely related to *apoptosis*, which is the process of programmed cell death that occurs in multicellular organisms and is widely known to be involved in un-controlled tumor growth in cancer. Another pathway involves the genes *BRCA1*, *BRCA2*, and *ATR*, which have all been associated with cancer susceptibility.

For comparison, we examine the genes selected with the ℓ_1 -norm penalty that does not consider the pathway information. In this case, we do not find any meaningful functional enrichment signals that are relevant to breast cancer. For example, among the 582 pathways that involve 687 genes at 37.55% error rate, we find two large pathways with functional enrichments, namely *response to organic substance* (83 genes with p -value $3.3E-13$) and the process of *oxidation reduction* (73 genes with p -value $1.7E-11$). However, both are quite large groups and matched to relatively high-level biological processes that do not provide much insight on cancer-specific pathways.

6. Conclusions

In this paper, we considered an optimization problem for estimating a structured-sparsity pattern in regression coefficients with a general class of structured-sparsity-inducing penalties. Many of the structured-sparsity-inducing penalties including the overlapping-group-lasso penalties and graph-guided fusion penalty share a common set of difficulties in optimization such as non-separability and non-smoothness. We showed that the optimization problems with these penalties can be transformed into the common form, and proposed a general optimization approach called smoothing proximal gradient method that can be applied to an optimization problem of this common form. Our results show that the proposed method can efficiently solve high-dimensional problems.

As for the future work, it is known that reducing μ over iterations leads to better empirical results. However, in such a scenario, the convergence rate is harder to analyze. In

addition, since the method is only based on gradient, its online version with the stochastic gradient descent can be easily derived. However, proving the regret bound will require a more careful investigation.

7. Appendix

7.1 Proof of Theorem 2

We first introduce the concept of *Fenchel Conjugate*.

Definition 9 *The Fenchel conjugate of a function $\varphi(\boldsymbol{\alpha})$ is the function $\varphi^*(\boldsymbol{\beta})$ defined as:*

$$\varphi^*(\boldsymbol{\beta}) = \sup_{\boldsymbol{\alpha} \in \text{dom}(\varphi)} (\boldsymbol{\alpha}^T \boldsymbol{\beta} - \varphi(\boldsymbol{\alpha})).$$

Recall that $d(\boldsymbol{\alpha}) = \frac{1}{2} \|\boldsymbol{\alpha}\|^2$ with the $\text{dom}(\boldsymbol{\alpha}) = \mathcal{Q}$. According to Definition 9, the conjugate of $d(\cdot)$ at $\frac{C\boldsymbol{\beta}}{\mu}$ is:

$$d^* \left(\frac{C\boldsymbol{\beta}}{\mu} \right) = \sup_{\boldsymbol{\alpha} \in \mathcal{Q}} \left(\boldsymbol{\alpha}^T \frac{C\boldsymbol{\beta}}{\mu} - d(\boldsymbol{\alpha}) \right),$$

and hence

$$f_\mu(\boldsymbol{\beta}) \equiv \arg \max_{\boldsymbol{\alpha} \in \mathcal{Q}} (\boldsymbol{\alpha}^T C\boldsymbol{\beta} - \mu d(\boldsymbol{\alpha})) = \mu d^* \left(\frac{C\boldsymbol{\beta}}{\mu} \right).$$

According to Theorem 26.3 in (Rockafellar, 1996) “a closed proper convex function is essentially strictly convex if and only if its conjugate is essentially smooth”, since $d(\boldsymbol{\alpha})$ is a closely proper strictly convex function, its conjugate is smooth. Therefore, $f_\mu(\boldsymbol{\beta})$ is a smooth function.

Now we apply Danskin’s Theorem (Prop B.25 in (Bertsekas, 1999)) to derive $\nabla f_\mu(\boldsymbol{\beta})$. Let $\phi(\boldsymbol{\alpha}, \boldsymbol{\beta}) = \boldsymbol{\alpha}^T C\boldsymbol{\beta} - \mu d(\boldsymbol{\alpha})$. Since $d(\cdot)$ is a strongly convex function, $\arg \max_{\boldsymbol{\alpha} \in \mathcal{Q}} \phi(\boldsymbol{\alpha}, \boldsymbol{\beta})$ has a unique optimal solution and we denote it as $\boldsymbol{\alpha}^*$. According to Danskin’s Theorem:

$$\nabla f_\mu(\boldsymbol{\beta}) = \nabla_{\boldsymbol{\beta}} \phi(\boldsymbol{\alpha}^*, \boldsymbol{\beta}) = C^T \boldsymbol{\alpha}^*. \quad (24)$$

As for the proof of Lipschitz constant of $f_\mu(\boldsymbol{\beta})$, readers may refer to (Nesterov, 2005).

7.2 Proof of Proposition 3

$$\begin{aligned} \boldsymbol{\alpha}^* &= \arg \max_{\boldsymbol{\alpha} \in \mathcal{Q}} \left(\boldsymbol{\alpha}^T C\boldsymbol{\beta} - \frac{\mu}{2} \|\boldsymbol{\alpha}\|_2^2 \right) \\ &= \arg \max_{\boldsymbol{\alpha} \in \mathcal{Q}} \sum_{g \in \mathcal{G}} \left(\gamma w_g \boldsymbol{\alpha}_g^T \boldsymbol{\beta}_g - \frac{\mu}{2} \|\boldsymbol{\alpha}_g\|_2^2 \right) \\ &= \arg \min_{\boldsymbol{\alpha} \in \mathcal{Q}} \sum_{g \in \mathcal{G}} \left\| \boldsymbol{\alpha}_g - \frac{\gamma w_g \boldsymbol{\beta}_g}{\mu} \right\|_2^2 \end{aligned} \quad (25)$$

Therefore, (25) can be decomposed into $|\mathcal{G}|$ independent problems: each one is the Euclidean projection onto the ℓ_2 -ball:

$$\boldsymbol{\alpha}_g^* = \arg \min_{\boldsymbol{\alpha}_g: \|\boldsymbol{\alpha}_g\|_2 \leq 1} \left\| \boldsymbol{\alpha}_g - \frac{\gamma w_g \boldsymbol{\beta}_g}{\mu} \right\|_2^2,$$

and $\boldsymbol{\alpha}^* = [(\boldsymbol{\alpha}_{g_1}^*)^T, \dots, (\boldsymbol{\alpha}_{g_{|\mathcal{G}|}}^*)^T]^T$.

According to the property of ℓ_2 -ball, it can be easily shown that:

$$\boldsymbol{\alpha}_g^* = S\left(\frac{\gamma w_g \boldsymbol{\beta}_g}{\mu}\right),$$

where $S(\mathbf{u}) = \begin{cases} \frac{\mathbf{u}}{\|\mathbf{u}\|_2} & \|\mathbf{u}\|_2 > 1, \\ \mathbf{u} & \|\mathbf{u}\|_2 \leq 1. \end{cases}$

As for $\|C\|$,

$$\begin{aligned} \|C\mathbf{v}\|_2 &= \gamma \sqrt{\sum_{g \in \mathcal{G}} \sum_{j \in g} (w_g)^2 v_j^2} \\ &= \lambda \sqrt{\sum_{j=1}^J \left(\sum_{g \in \mathcal{G} \text{ s.t. } j \in g} (w_g)^2 \right) v_j^2}, \end{aligned}$$

the maximum value of $\|C\mathbf{v}\|_2$, given $\|\mathbf{v}\|_2 \leq 1$, can be achieved by setting v_j for j corresponding to the largest summation $\sum_{g \in \mathcal{G} \text{ s.t. } j \in g} (w_g)^2$ to one, and setting other v_j 's to zeros. Hence, we have

$$\|C\mathbf{v}\|_2 = \gamma \max_{j \in \{1, \dots, J\}} \sqrt{\sum_{g \in \mathcal{G} \text{ s.t. } j \in g} (w_g)^2}.$$

7.3 Proof of Proposition 4

Similar to the proof technique of Proposition 1, we reformulate the problem of solving $\boldsymbol{\alpha}^*$ as a Euclidean projection:

$$\begin{aligned} \boldsymbol{\alpha}^* &= \arg \max_{\boldsymbol{\alpha} \in \mathcal{Q}} \left(\boldsymbol{\alpha}^T C \boldsymbol{\beta} - \frac{\mu}{2} \|\boldsymbol{\alpha}\|_2^2 \right) \\ &= \arg \min_{\boldsymbol{\alpha}: \|\boldsymbol{\alpha}\|_\infty \leq 1} \left\| \boldsymbol{\alpha} - \frac{C\boldsymbol{\beta}}{\mu} \right\|_2^2, \end{aligned}$$

and the optimal solution $\boldsymbol{\alpha}^*$ can be obtained by projecting $\frac{C\boldsymbol{\beta}}{\mu}$ onto the ℓ_∞ -ball.

According to the construction of matrix C , we have for any vector \mathbf{v} :

$$\|C\mathbf{v}\|_2^2 = \gamma^2 \sum_{e=(m,l) \in E} (\tau(r_{ml}))^2 (v_m - \text{sign}(r_{ml})v_l)^2 \quad (26)$$

By the simple fact that $(a \pm b)^2 \leq 2a^2 + 2b^2$ and the inequality holds as equality if and only if $a = \pm b$, for each edge $e = (m, l) \in E$, the value $(v_m - \text{sign}(r_{ml})v_l)^2$ is upper bounded

by $2v_m^2 + 2v_l^2$. Hence, when $\|\mathbf{v}\|_2 = 1$, the right-hand side of (26) can be further bounded by:

$$\begin{aligned}
 \|C\mathbf{v}\|_2^2 &\leq \gamma^2 \sum_{e=(m,l) \in E} 2(\tau(r_{ml}))^2 (v_m^2 + v_l^2) \\
 &= \gamma^2 \sum_{j \in V} (\sum_{e \text{ incident on } j} 2(\tau(r_e))^2) v_j^2 \\
 &= \gamma^2 \sum_{j \in V} 2d_j v_j^2 \\
 &\leq 2\gamma^2 \max_{j \in V} d_j,
 \end{aligned} \tag{27}$$

where

$$d_j = \sum_{e \in E \text{ s.t. } e \text{ incident on } j} (\tau(r_e))^2.$$

Therefore, we have

$$\|C\| \equiv \max_{\|\mathbf{v}\|_2 \leq 1} \|C\mathbf{v}\|_2 \leq \sqrt{2\gamma^2 \max_{j \in V} d_j}.$$

Note that this upper bound is tight because the first inequality in (27) is tight.

7.4 Proof of Theorem 7

This proof follows the similar scheme used in (Lan et al., 2011). Based on the result from (Beck and Teboulle, 2009), we have the following lemma:

Lemma 10 *For the function $\tilde{f}(\boldsymbol{\beta}) = h(\boldsymbol{\beta}) + \lambda\|\boldsymbol{\beta}\|_1$, where $h(\boldsymbol{\beta})$ is an arbitrary convex smooth function and its gradient $\nabla h(\boldsymbol{\beta})$ is Lipschitz continuous with the Lipschitz constant L . We apply Algorithm 1 to minimize $\tilde{f}(\boldsymbol{\beta})$ and let $\boldsymbol{\beta}^t$ be the approximate solution at the t -th iteration. For any $\boldsymbol{\beta}$, we have the following bound:*

$$\tilde{f}(\boldsymbol{\beta}^t) - \tilde{f}(\boldsymbol{\beta}) \leq \frac{2L\|\boldsymbol{\beta} - \boldsymbol{\beta}^0\|_2^2}{t^2}. \tag{28}$$

In order to use the bound in (28), we decompose $f(\boldsymbol{\beta}^t) - f(\boldsymbol{\beta}^*)$ into three terms:

$$f(\boldsymbol{\beta}^t) - f(\boldsymbol{\beta}^*) = \left(f(\boldsymbol{\beta}^t) - \tilde{f}(\boldsymbol{\beta}^t) \right) + \left(\tilde{f}(\boldsymbol{\beta}^t) - \tilde{f}(\boldsymbol{\beta}^*) \right) + \left(\tilde{f}(\boldsymbol{\beta}^*) - f(\boldsymbol{\beta}^*) \right). \tag{29}$$

According to the definition of \tilde{f} , we know that for any $\boldsymbol{\beta}$

$$\tilde{f}(\boldsymbol{\beta}) \leq f(\boldsymbol{\beta}) \leq \tilde{f}(\boldsymbol{\beta}) + \mu D,$$

where $D \equiv \max_{\boldsymbol{\alpha} \in \mathcal{Q}} d(\boldsymbol{\alpha})$. Therefore, the first term in (29), $f(\boldsymbol{\beta}^t) - \tilde{f}(\boldsymbol{\beta}^t)$, is upper-bounded by μD , and the last term in (29) is less than or equal to 0 (i.e., $\tilde{f}(\boldsymbol{\beta}^*) - f(\boldsymbol{\beta}^*) \leq 0$). Combining (28) with these two simple bounds, we have:

$$f(\boldsymbol{\beta}^t) - f(\boldsymbol{\beta}^*) \leq \mu D + \frac{2L\|\boldsymbol{\beta}^* - \boldsymbol{\beta}^0\|_2^2}{t^2} \leq \mu D + \frac{2\|\boldsymbol{\beta}^* - \boldsymbol{\beta}^0\|_2^2}{t^2} \left(\lambda_{\max}(\mathbf{X}^T \mathbf{X}) + \frac{\|C\|^2}{\mu} \right). \tag{30}$$

By setting $\mu = \frac{\epsilon}{2D}$ and plugging this into the right-hand side of (30), we obtain

$$f(\boldsymbol{\beta}^t) - f(\boldsymbol{\beta}^*) \leq \frac{\epsilon}{2} + \frac{2\|\boldsymbol{\beta}^* - \boldsymbol{\beta}^0\|_2^2}{t^2} \left(\lambda_{\max}(\mathbf{X}^T \mathbf{X}) + \frac{2D\|C\|^2}{\epsilon} \right). \tag{31}$$

If we require the right-hand side of (31) to be equal to ϵ and solve it for t , we obtain the bound of t in (18).

Acknowledgements

We would like to thank Yanjun Qi for the help of preparation and verification of breast cancer dataset. We would also like to thank Javier Peña for the helpful discussion of the related first-order methods.

References

- The MOSEK Optimization Software* (<http://www.mosek.com/>).
- N. Abate, M. Chandalia, P. Satija, B. Adams-Huet, and et. al. Enpp1/pc-1 k121q polymorphism and genetic susceptibility to type 2 diabetes. *Diabetes*, 54(4):1027–1213, 2005.
- A. Beck and M. Teboulle. A fast iterative shrinkage thresholding algorithm for linear inverse problems. *SIAM Journal of Image Science*, 2(1):183–202, 2009.
- Dimitri Bertsekas. *Nonlinear Programming*. Athena Scientific, 1999.
- John Duchi and Yoram Singer. Efficient online and batch learning using forward backward splitting. *Journal of Machine Learning Research*, 10:2899–2934, 2009.
- Jerome Friedman, Trevor Hastie, Holger Höfling, and Robert Tibshirani. Pathwise coordinate optimization. *Annals of Applied Statistics*, 1:302–332, 2007.
- Holger Hoefling. A path algorithm for the fused lasso signal approximator. Technical report, arXiv:0910.0526v1 [stat.CO], 2009.
- Da Wei Huang, Brad T Sherman, and Richard A Lempicki. Systematic and integrative analysis of large gene lists using david bioinformatics resources. *Nature Protoc*, 4(1):44–57, 2009.
- Laurent Jacob, Guillaume Obozinski, and Jean-Philippe Vert. Group lasso with overlap and graph lasso. In *ICML*, 2009.
- Rodolphe Jenatton, Jean-Yves Audibert, and Francis Bach. Structured variable selection with sparsity-inducing norms. Technical report, INRIA, 2009.
- Rodolphe Jenatton, Julien Mairal, Guillaume Obozinski, and Francis Bach. Proximal methods for sparse hierarchical dictionary learning. In *ICML*, 2010.
- Seyoung Kim and Eric P. Xing. Tree-guided group lasso for multi-task regression with structured sparsity. In *ICML*, 2010.
- Seyoung Kim, Kyung-Ah Sohn, and Eric P. Xing. A multivariate regression approach to association analysis of a quantitative trait network. *Bioinformatics*, 25(12):204–212, 2009.
- G. Lan, Z. Lu, and R.D.C. Monteiro. Primal-dual first-order methods with $\mathcal{O}(1/\epsilon)$ iteration complexity for cone programming. *Mathematical Programming*, 126:1–29, 2011.
- J. Liu and J. Ye. Fast overlapping group lasso. Technical report, ArXiv:1009.0306v1 [cs.LG], 2010a.

- J. Liu and J. Ye. Moreau-yosida regularization for grouped tree structure learning. In *NIPS*, 2010b.
- Jun Liu, Shuiwang Ji, and Jieping Ye. Multi-task feature learning via efficient $\ell_{2,1}$ -norm minimization. In *UAI*, 2009.
- Jun Liu, Lei Yuan, and Jieping Ye. An efficient algorithm for a class of fused lasso problems. In *the 16th ACM SIGKDD*, 2010.
- Shuangge Ma and Michael R Kosorok. Detection of gene pathways with predictive power for breast cancer prognosis. *BMC Bioinformatics*, 11(1), 2010.
- J. Mairal, R. Jenatton, G. Obozinski, and F. Bach. Network flow algorithms for structured sparsity. In *NIPS*, 2010.
- S. Mosci, S. Villa, A. Verri, and L. Rosasco. A primal-dual algorithm for group sparse regularization with overlapping groups. In *NIPS*, 2010.
- Yurii Nesterov. Excessive gap technique in non-smooth convex minimization. Technical report, Universit catholique de Louvain, Center for Operations Research and Econometrics (CORE), 2003.
- Yurii Nesterov. Smooth minimization of non-smooth functions. *Mathematical Programming*, 103(1):127–152, 2005.
- Yurii Nesterov. Gradient methods for minimizing composite objective function. Technical report, ECOPE, 2007.
- Guillaume Obozinski, Ben Taskar, and Michael I. Jordan. High-dimensional union support recovery in multivariate regression. In *NIPS*, 2009.
- R.T. Rockafellar. *Convex Analysis*. Princeton Univ. Press, 1996.
- A. Subramanian, P. Tamayo, V. Mootha, and et. al. Gene set enrichment analysis: A knowledge-based approach for interpreting genome-wide expression profiles. *Proceedings of the National Academy of Sciences*, 102(43):15545–15550, 2005.
- The International HapMap Consortium. A haplotype map of the human genome. *Nature*, 437:1399–1320, 2005.
- R. J. Tibshirani and J. Taylor. The solution path of the generalized lasso. Technical report, arXiv:1005.1971v2 [math.ST], 2010.
- Robert Tibshirani. Regression shrinkage and selection via the lasso. *Journal of the Royal Statistical Society: Series B*, 58:267–288, 1996.
- Robert Tibshirani and Michael Saunders. Sparsity and smoothness via the fused lasso. *Journal of the Royal Statistical Society, Series B*, 67(1):91–108, 2005.
- Reha H. Tütüncü, Kim C. Toh, and Michael J. Todd. Solving semidefinite-quadratic-linear programs using sdpt3. *Mathematical Programming*, 95:189–217, 2003.

Marc J. van de Vijver et al. A gene-expression signature as a predictor of survival in breast cancer. *New England Journal of Medicine*, 347:1999–2009, 2002.

Ming Yuan and Yi Lin. Model selection and estimation in regression with grouped variables. *Journal of the Royal Statistical Society: Series B*, 68:49–67, 2006.

Peng Zhao, Guilherme Rocha, and Bin Yu. The composite absolute penalties family for grouped and hierarchical variable selection. *The Annals of Statistics*, 37(6A):3468–3497, 2009.